Appl Phys A (2013) 111:1–8
DOI 10.1007/s00339-012-7534-x

Applied Physics A
Materials Science & Processing

High-resolution fluorescence mapping of impurities in historical zinc oxide pigments: hard X-ray nanoprobe applications to the paints of Pablo Picasso

Francesca Casadio · Volker Rose

Received: 5 August 2012 / Accepted: 26 December 2012 / Published online: 24 January 2013

Abstract Here for the first time we describe the use of high resolution nanoprobe X-ray fluorescence (XRF) mapping for the analysis of artists' paints, hierarchically complex materials typically composed of binder, pigments, fillers, and other additives. The work undertaken at the nanoprobe sought to obtain highly spatially resolved, highly sensitive mapping of metal impurities (Pb, Cd, Fe, and other metals) in submicron particles of zinc oxide pigments used in early 20th century artists' tube paints and enamel paints, with particular emphasis on Ripolin, a popular brand of French house paint used extensively by Pablo Picasso and some of his contemporaries. Analysis revealed that the Zn oxide particles only contain a little Fe, proving that the highest quality Zn oxide pigment, free of Pb and Cd, was used for Ripolin house paints as well as artists' paints. Nanoprobe XRF mapping also demonstrated that artists' tube paints generally have more abundant fillers and additional whites (based on Pb, Ti, Ca) than Ripolin paints, which contain mostly pure zinc oxide. The chemical characterization of paints at the nanoscale opens the path to a better understanding of their fabrication and chemical reactivity.

1 Introduction

The detailed characterization of artists' paints and industrial coatings—hierarchically complex materials typically composed of binder, pigments, fillers and other additives—presents a multiscale challenge. Techniques for the characterization and mapping of inorganic paint components at multiple length scales are well established, but until the present day high-sensitivity measurements with submicron resolution were scarcely available (Fig. 1). For example, fiber-optics reflectance spectroscopy (FORS, 350 to 2500 nm) and hyper-spectral imaging have been demonstrated to resolve and map multiple pigments on entire paintings, probing the meter and cm scales easily and effectively [1]. At the mm scale, X-ray fluorescence spectroscopy and mapping with portable systems have been extensively used [2, 3], and recently the possibility to map pigment distribution over entire paintings has also been described [4]. Scanning electron microscopy with energy dispersive X-ray spectroscopy (SEM/EDX) is well established as a routine tool in cultural heritage research to map pigment distribution within cross sections of paintings at micrometer-scale resolution; and in the last few decades, Fourier Transform Infrared (FTIR) [5], Raman and FT-Raman microspectroscopies have offered similar capabilities for molecular mapping [6–8]. Synchrotron-based techniques such as micro-X-ray diffraction (XRD) and micro-X-ray absorption near-edge spectroscopy (XANES) are also increasingly used to probe original components and degradation products in cross sections from paintings and other samples [9–11]. Until now, however, it was not possible to visualize elemental composition and nanoscale distribution of elements within individual submicrometric pigment particles, which, in the case of zinc-oxide-based paints, have diameters typically ranging between 200 nm and 1 μm [12]. Thus, the question remained whether impurities identified in the chemical analysis of paints were located in the binding matrix or within

F. Casadio (✉)
The Art Institute of Chicago, Chicago, IL 60603, USA
e-mail: fcasadio@artic.edu

V. Rose
Advanced Photon Source and Center for Nanoscale Materials, Argonne National Laboratory, Argonne, IL 60439, USA

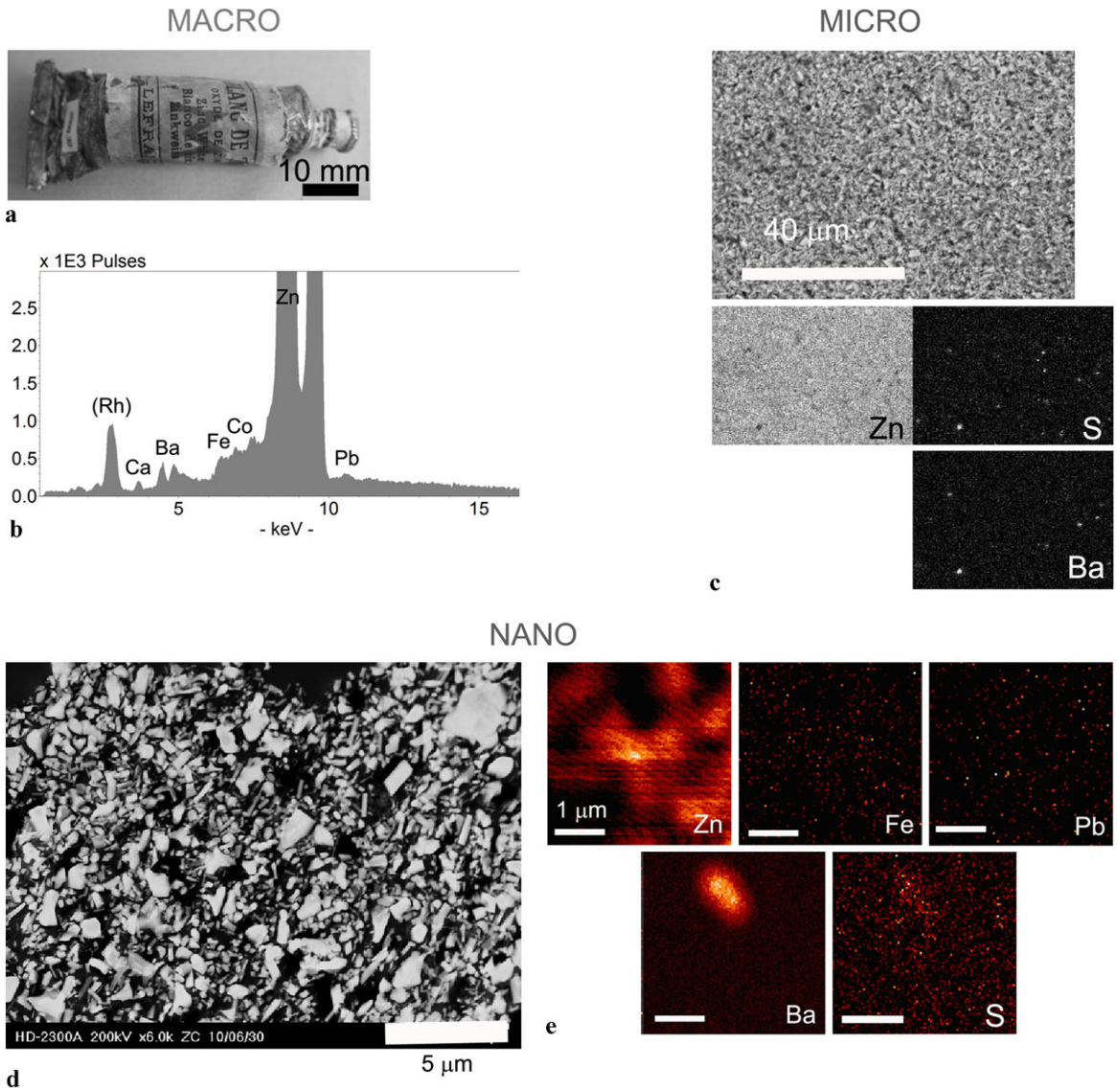

Fig. 1 Hierarchical paint characterization from cm to nm: (**a**) undated historic tube of Lefranc zinc white artists' oil paint labeled "Blanc de Zinc" (2009.32); (**b**) bulk XRF spectrum of the paint from the tube (approximate area analyzed is 8 mm in diameter); (**c**) Backscattered scanning electron microscope image of a sample of the white paint from (**a**) and elemental maps showing the distribution of Zn, S, Ba (area scanned is 100 µm wide); (**d**) Scanning Transmission Electron Micrograph of a thin section (250-nm thick by 20-µm wide) of the white paint from (**a**); (**e**) nano-XRF maps showing spatial distribution of elements within the same paint, over a 3×3 µm^2 area

the ZnO pigment particles themselves. Recent experiments at the Hard X-Ray Nanoprobe of the Advanced Photon Source at Argonne National Laboratory allowed breaking this barrier. This next generation hard X-ray microscopy and imaging system combines superior spatial resolution (down to 30 nm) with very high elemental sensitivity [13] allowing the visualization of unprecedented information within a single grain of pigment.

Here the compositional study of zinc oxide pigments used in early 20th century artists' tube paints and enamel paints is described. The motivation for this work is twofold: firstly, the capability of mapping metal impurities within pigment particles might prove helpful in distinguishing different manufacturing routes and providing an increased understanding of their chemical reactivity. Secondly, recent interest in the different range of luminescence properties of various zinc-based white pigments [14, 15], and the extensive knowledge-base on the effects of metal impurities, particle size and shape on the photoluminescence of ZnO nanoparticles [16] suggest that achieving spatial correlation of impurities with ZnO nanoparticles of different origins and productions may be extremely useful to better understand the observed modifications to the electronic structure of this wide band semiconductor.

1.1 Pablo Picasso and Ripolin paints

Although known since the previous century, white paints based on zinc oxide became commercially significant only in the mid-19th century, when formulations with good hiding power in oil and acceptable drying times due to the addition of suitable driers were achieved [17]. France was an early adopter of zinc white for house paints because of toxicity concerns with lead white (basic lead carbonate, or hydrocerussite, $2PbCO_3{\cdot}Pb(OH)_2$), and the need for paint coatings that would not darken when exposed to the polluted atmospheres of the times, which were rich in sulphurous gases. Legislation dating back to at least 1909 banned the use of lead white in France for certain applications [18]. Messrs. Leclaire & Co of Paris have been traditionally credited with discovering zinc paint [19]. One of the first commercial companies to manufacture high-quality zinc-oxide enamel paints on a large scale was the Ripolin company, established in 1897 at the outskirts of Paris through the merger of a Dutch enterprise and the French firm Lefranc, the renowned manufacturer of artists' materials [20]. Ripolin paints quickly rose to remarkable fame and held a stable market dominance position for several decades, leading to the frequent use of "ripolin" as synonymous term with enamel paints in general.

One of the early adopters of this household enamel paint for artistic uses was Pablo Picasso (1881–1973), quickly followed by many other avant-garde artists of his time [20]. Picasso's painting practices marked a radical departure from those of his predecessors because of his pioneering introduction of industrial, commonplace materials into the fine art studio. Ripolin provided quick drying paints that rendered brushless, glossy, enamel-like surfaces in a range of bright colors, with good covering power, effects that were difficult to achieve with artists' paint tubes. Picasso used Ripolin paints starting as early as 1912 and continued their use throughout his long and productive career, alongside other brands of house paints and artists' paints [21, 22].

Because the main components of these bio-based resins are triglyceride oils (mostly stand-oil, or prepolymerized, heat-treated oil) and natural resin varnishes, these systems have often been referred to as oleoresinous paints. Before 1950, white Ripolin paints produced in France were typically composed of zinc oxide with only trace amounts of fillers or extenders (only sporadic traces of barium sulfate have been detected in formulations throughout the years). Because of the fine and extensive grinding process undergone by the paints, the pigment had extremely small particle size (with high concentration of particles in the 150–300 nm length/diameter range) and a very limited presence of acicular zinc oxide crystals [21]. In the mature paints, products of the interaction of ZnO and the oleoresinous medium are present, as well as other organometallic salts of cobalt, manganese, lead, and possibly zinc used as paint driers. Given that both artists' and industrial paints were based on oleoresinous media before 1950, in many cases not even a complete chemical analysis can uniquely identify and distinguish all their components [22], and presently only particle size analysis appears to successfully distinguish between the two types.

The nanoprobe investigation described in this work allowed testing different types of historic zinc oxide pigments to establish the nature and abundance of metallic impurities for both artists' and household Ripolin paints.

1.2 Historical production of zinc oxide for paints and coatings in the early 20th C

The historical technical literature documents two main manufacturing processes available in the early 20th century that produced zinc oxide pigments of variable purity and quality. The French (also called *indirect*) process used metallic zinc as starting material, boiling the metal in contact with air and collecting the resulting oxide [23, 24]. The American (*direct*) process used franklinite as starting material, a natural ore of zinc carbonate, which was roasted in air together with a carbonaceous reducing agent such as coal.

The pigment was sold in different grades, containing varying levels of impurities. The main impurities were typically Cd, Pb, Sb, Fe, S in amounts ranging between 0.2 to over 1 w% [17, 25]. Cd was considered particularly detrimental as its colored oxides would diminish the whiteness of the zinc oxide pigment [23]. For the indirect process, the finest pigment grade was termed "White seal" and was derived from electrolytic zinc, free from associated metals, as starting material. It had a slight bluish cast and was used for pharmaceutical purposes and also for the finest quality of full gloss house paints: it was entirely free of Pb and with impurities not exceeding 0.2 w%. "Green and Red seal" zinc whites, mostly used in paint manufactory, had approximately 1 w% impurities, consisting mainly of Pb, with traces of Cd, Fe, and Sb, which imparted a slight yellowish tinge to the final product. "Blue and Yellow seal" were the lowest, most impure grades. The direct process oxide tended to be more impure and generally contained small amounts of Pb as the basic sulfate, ranging from 1 up to 4 w%.

2 Experimental details

2.1 Paint samples

The samples analyzed were drawn from an extensive reference collection of mainly French house- and artists' paints from the first half of the 20th century housed at the Art Institute of Chicago (AIC) [20]. The nanoprobe survey investigated four examples of artists' tube paints by noted

French manufacturers Lefranc and Lefebvre Foinet, as well as Dutch manufacturer Claus and Fritz, along with a sample of present-day chemical grade zinc oxide (Sigma Aldrich). Four samples of enamel paints of Ripolin production and two of American production were also investigated, as well as five samples from paintings by Pablo Picasso and Francis Picabia. The subset described here includes representative examples within this larger group. Specifically: white paints from a swatch of *Blanc de neige #1* of a Ripolin paint color chart datable between 1929 and 1946 (AIC reference number B02), as well as a sample of *Gloss white paint* (AIC ref. n. HP031) of Ripolin paint of American production, generously provided by the National Gallery, Washington, DC, USA, are described in detail. The latter paint is the only one in alkyd medium, which dates the paint after the mid-1930s, when alkyds were first introduced. Two different undated historic tubes of Lefranc zinc white artists' oil paints were also analyzed and are described herein, a tube labeled "pour decoration artistique" (AIC ref. n. 2007.48) and one of "Blanc de Zinc" (2009.32). Finally, a sample of white paint and ground from a painting by Pablo Picasso that was suspected to contain Ripolin paints is also described [19]. The painting is entitled *Nature morte aux trois poissons, à la murène, au citron vert sur fond blanc* (*Still Life with Three Fish, Moray Eel and Lime on White Ground*, oleoresinous enamel paint and charcoal on reused canvas, 38 × 55 cm, MPA 1946.1.15), is dated 28 September 1946 and is part of the collection of the Musée Picasso, Antibes, France.

2.2 Hard X-ray nanoprobe

Experiments were carried out at the Center for Nanoscale Materials Hard X-ray Nanoprobe instrument, which is operated on ID-26 at the Advanced Photon Source, Argonne National Laboratory [26]. The instrument uses two collinear undulators as photon source, a Si(111) double-crystal monochromator to select the X-ray energy, and Fresnel zone plate optics for focusing of X-rays onto the sample. The selected photon energy was 10 keV. X-ray fluorescence from the sample was detected with a four-element silicon drift energy dispersive detector. The sample was located in a high-vacuum chamber (10^{-6} torr) in order to reduce air scattering and absorption. Fluorescence data have been analyzed using the software package MAPS [27]. Fitting and quantification of the fluorescence data was carried out with thin film standards (National Bureau of Standards, Standard Reference Material 1832 and 1833). Absolute concentrations of elements could be calculated by fitting the experimental spectra versus those of the standard materials, after normalization by incoming photon flux. The high-energy synchrotron X-ray beam enables sensitivities three orders of magnitude higher than scanning electron microscope work, leading to sub-ppm sensitivity, which increases with atomic number (Z). For example, the detection limit for Zn has been measured to be 4 atto-gram for 1 s acquisition time and a 0.2 × 0.2 μm^2 spot with a 200 nm zone plate at the microprobe [28]. Because in the experiments described here a 30 nm zone plate was used, a detection limit of about 200 atto-gram can be extrapolated for Zn considering a comparable flux density. Furthermore, the high resolution of the nanoprobe together with the precise fitting allowed us to correctly quantify the contributions due to the Co Kα (at 6.931 keV) and from the escape peak of Zinc (at 6.897 keV), which are very close in energy. Although absolute concentrations were measured, most results are reported as ratios of elements so as to allow better inter-comparison of samples with different thicknesses.

The high-energy beam footprint of the synchrotron hard-x ray nanoprobe allowed relatively rapid acquisition of maps of 3 × 3 μm^2 areas in different regions of the samples separated by macroscopic distances relatively quickly, so as to provide statistically meaningful high-resolution measurements. That the results obtained at the nanoscale are representative of the entirety of the samples was also appropriately supported by previous measurements carried out with macro X-Ray Fluorescence (XRF), Scanning Electron Microscopy with Energy Dispersive X-ray Spectrometry (SEM/EDX), Fourier Transform Infrared Spectroscopy (FTIR), and Laser Ablation Inductively Coupled Plasma Emission Mass Spectrometry (LA-ICP/MS) [21, 22].

3 Results and discussion

A high-resolution scanning transmission electron microscopy image (STEM) of a sample from the Ripolin paint color swatch *Blanc de neige #1* illustrates the typical particle morphology and wide-spaced distribution of zinc white pigment particles in Ripolin paints (Fig. 2). Previous macro-XRF measurements of the sample revealed an overall composition dominated by Zn, with traces of Pb, Co, and some Fe, while micro-FTIR analysis confirmed the presence of zinc oxide and organometallic soaps in a drying oil medium. Several 3 × 3 μm^2 areas of this sample were analyzed with the X-ray nanoprobe with a 30-nm step size: the maps showed that the Fe distribution follows very closely the regions with zinc oxide particles, with excellent correlation after normalization to remove background effects. Analysis also revealed rare, isolated particles of titanium dioxide, which were not detected by macro-XRF (Fig. 3). Concentrations of elements in the various high-resolution maps could be determined by means of the fitted and normalized data from measurements of NIST standard reference materials 1832 and 1833 and are reported as maximum and minimum values measured over the entire 3 × 3 μm^2 imaged area. In the area depicted in Fig. 3, such quantitative compositional

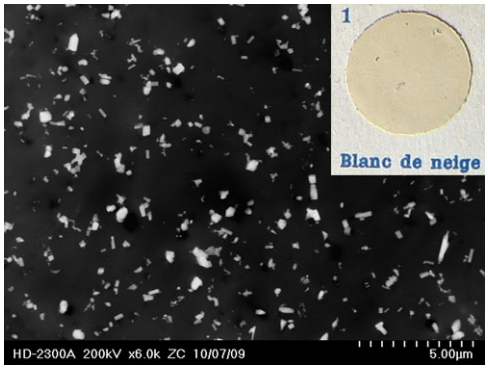

Fig. 2 Scanning Transmission Electron micrograph of a thin section (250-nm thick by 20-µm wide) of the white paint from a Ripolin color chart (*Blanc de neige #1*; B02, shown in the *inset*). The very minute, mostly globular and often submicrometric particles of zinc oxide are evident

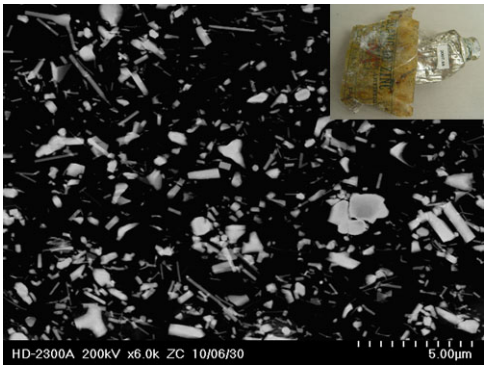

Fig. 4 Scanning Transmission Electron micrograph of a thin section (250-nm thick by 20-µm wide) of the white paint from an historic tube of Lefranc zinc white artists' oil paint (shown in the *inset*) labeled "pour decoration artistique" (AIC ref. n. 2007.48). The image highlights the dense distribution of both small and large particles, with an abundance of acicular particles

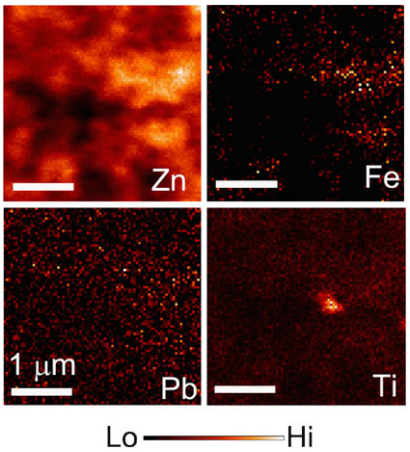

Fig. 3 Nano-XRF maps of a 3 × 3 µm^2 region in a sample of Ripolin *Blanc de neige* #1 from color chart B02, highlighting the correlation of Zn with Fe, the presence of occasional particles of Ti white and the absence of well-defined Pb-rich particles

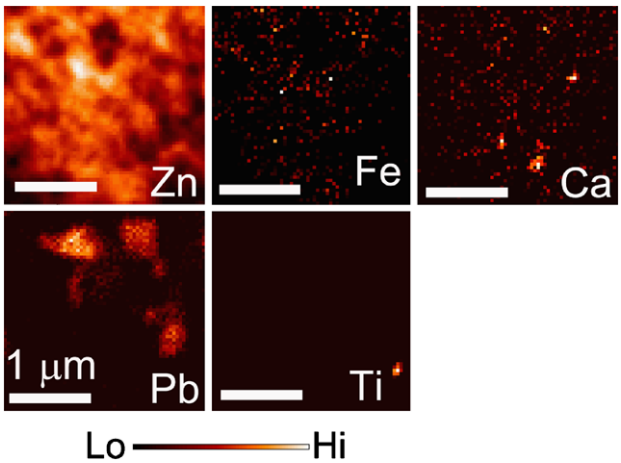

Fig. 5 Nano-XRF maps of a 3 × 3 µm^2 region in a sample of Lefranc zinc white artists' oil paint (2007.48) showing the presence of discrete particles of Ca-rich extenders as well as Pb- and Ti-based whites

analysis indicated ranges of zinc concentrations from a maximum of 1050 µg/cm^2 measured within the pigment particles, to a minimum of 480 µg/cm^2 measured in the binder; to be compared with levels of max 3.2 µg/cm^2 and min 0.80 µg/cm^2 for Fe. Furthermore, while some Pb was detected in the sum-XRF spectra obtained with the nanoprobe (ranging from 41.4 to 0 µg/cm^2), Pb maps did not show clusters of well-defined particles. This suggests that the Pb is present in the paints in the form of lead-carboxylate driers, rather than as the pigment lead white (an inference supported by the fact that FTIR analysis did not detect any lead white).

A STEM image for the artist's tube paint (2007.48 Lefranc Blanc de zinc pour decoration artistique) illustrates the higher density of pigment particles in the binder matrix, as well as the generally larger particle size and more frequent occurrence of acicular, elongated pigment particles, when compared to the Ripolin sample (Fig. 4). Nano-XRF mapping detected a weaker, but still convincing correlation between the Fe and Zn distribution, while also highlighting the presence of large and widespread particles of lead-based pigment as well as some calcium-based particles and occasional titanium-based ones (Fig. 5). Because this sample was much thinner than the previous one, measured area concentrations for the elements of interest are lower than for the previous sample, given that at 10 keV the attenuation length of the synchrotron X-ray beam in Zn is about 10 µm [29]. Measured concentrations for Zn in the 3 × 3 µm^2 area illustrated in Fig. 5 ranged between 315 and 135 µg/cm^2, with values of 0.5–0.2 µg/cm^2 for Fe and 75.6–0 µg/cm^2 for Pb. On the mm-size scale, previous macro-XRF analysis of this sample also revealed higher counts for the Pb peaks, when compared to spectra of the B02-#1 Ripolin paint, and hydrocerussite was unambiguously identified with micro-

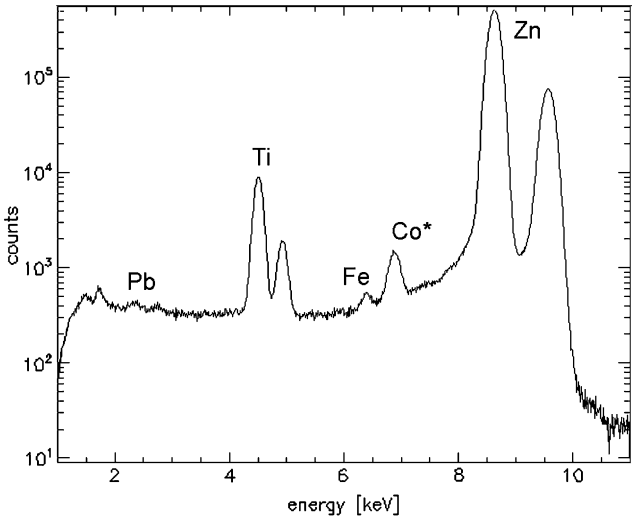

Fig. 6 XRF spectrum, integrated over the entire 3 × 3 μm^2 area illustrated in Fig. 7, for a sample of white gloss paint from a can of American Ripolin (HP031). The *asterisk* indicates that part of the intensity measured for the Co peak is in actuality due to the escape peak for zinc

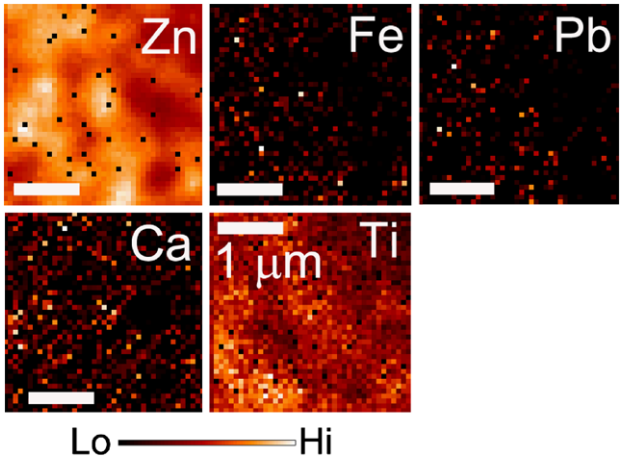

Fig. 7 Nano-XRF maps of a 3 × 3 μm^2 region in a sample of white gloss paint from a can of American Ripolin (HP031) showing enrichment in Pb of areas where the Zn particles are, and the presence of particles of white pigment rich in Ti

FTIR analysis, in addition to zinc white, zinc stearate, and other metallic carboxylates in a drying oil-based binder. The tube of higher-quality artist's paint (AIC ref. n. 2009.32) was shown by nano-XRF mapping to have fewer additives, with only occasional large particles of natural barium sulfate present and fair spatial correlation between the Fe distribution and the localization of the ZnO particles (Fig. 1). Absolute elemental concentrations across the whole 3 × 3 μm^2 area imaged (Fig. 1e) ranged between 462–385 μg/cm^2 for Zn, to 0.7–0.3 μg/cm^2 for Fe. In this case too, although Pb was detected (max 7.71 to 0 μg/cm^2), no distinct particles of lead-based pigments were evidenced by the nano-XRF mapping. At the macro (mm) scale, hand-held XRF previously identified major Zn with small amounts of Ba, Co, and traces of Pb, while FTIR microspectroscopy confirmed zinc oxide in oil with some metal stearate and other metal carboxylates. The sample of a can of American Ripolin (HP031) showed a very different composition and nanoscale distribution of elements, when compared to the French produced one (Fig. 6). Firstly, titanium white particles were detected as whitening agent, used in addition to ZnO. The Fe distribution clearly matches the regions where ZnO particles are present; furthermore, some small particles of Ca-based white were also highlighted. Although the Pb seems to be rather widespread in the area analyzed, spots with higher concentrations were evidenced in correspondence with areas of ZnO particles (Fig. 7). Measured elemental concentrations for the sample ranged between 9100 and 143 μg/cm^2 for Zn, 40.6 and 0 μg/cm^2 for Fe, 700 and 300 μg/cm^2 for Pb, and 700 and 5 μg/cm^2 for Ti for the area illustrated in Fig. 7. At the macroscale, macro-XRF did confirm the presence of high levels of Zn and Ti, with trace Fe, Co, and Pb, while previous FT-Raman analysis clarified the nature of the Ti and Ca-based pigments as anatase and calcite, respectively, with traces of lead white. The amount of lead white detected with previous FTIR and FT-Raman measurements is extremely low, when compared to the widespread Pb presence mapped with the nanoprobe, which seems to suggest that only a minimal portion of Pb is present as the pigment lead white, while a significant part, especially the one correlating well with the Zn distribution, might be considered an impurity of the Zn white used in these paints.

In order to compare values for elemental concentrations measured for samples of different thicknesses the MAPS software was used to isolate a region of interest centered on similar-size zinc oxide particles and calculate ratios of elemental concentrations (μg/cm^2) within the chosen particle. Rationing the concentration of Fe/Zn over a ZnO particle for each type of paint gave values of 0.0026 for B02-01, 0.0020 for American Ripolin, 0.0014 for 2007.48, and 0.0013 for 2009.32. This trend of slightly higher Fe/Zn content for Ripolin paints with respect to Lefranc tube paints was confirmed also by complementary measurements on the same paints with LA-ICP/MS (results not shown).

High-resolution maps on the Picasso sample of white house paint revealed a strong correlation between the distributions of Fe and Zn, also evidencing particles of calcium-based white and barium sulphate (Fig. 8). The latter are due to the painting's ground layer, which lies below the suspected Ripolin paint layer (Fig. 9). Because the interaction volume of the hard synchrotron X-ray beam extends for multiple microns depending on the material, with actual samples from paintings, it is often the case that the XRF maps reflect the composition of multiple layers. In fact, differently from the reference samples, samples from actual paintings

rarely consist of a single layer of paint (Fig. 9). In the particular conditions used for these experiments, it is estimated that, with photon energy of 10 keV (i.e., close to the element's absorption edge), the penetration depth in Zn is approximately 10 μm [29]. Complementary FTIR analysis of the ground layer of this paintings confirmed a composition based on zinc oxide, calcium carbonate, kaolin, and barium sulfate, which allows us to interpret the nanoprobe Ca and Ba maps as pertaining to the ground, and not to the paint layer.

4 Conclusions

The full chemical characterization of artists' paints requires a variety of analytical techniques with resolution at multiple length scales. This work demonstrates that high-resolution, high-sensitivity XRF nanoprobe techniques can effectively map and localize impurities within submicrometric pigment particles. Compared with traditional techniques of elemental analysis and mapping, such as SEM/EDX, the XRF nanoprobe allows us to obtain data with high spatial resolution and about 10^3 times higher sensitivity. Although the two techniques should be considered complementary parts of a multiscale analysis of paint components, the XRF nanoprobe for the first time enables the acquisition of compositional maps reflecting the distribution of impurities within a single pigment particle, as well as the detection of very small, albeit statistically significant, chemical differences. Also, extensive sample preparation that could introduce artifacts is not required for nano-XRF. Measurements on historical samples of zinc-oxide-based French paints demonstrated that the pigments used have no Cd or Pb impurities at the nanoscale. In essence, the experiments demonstrated that similar French process ZnO of the highest quality and purity was used for both house paints as well as artists' paints manufactured in France. In fact, only a little Fe was detected within the ZnO particles. The current experiments showed slightly higher Fe content for French Ripolin zinc oxide with respect to that of tube paints, but more samples will need to be evaluated in the future, to ensure reliable statistical representation. Artists' paint tubes were also shown to have more abundant fillers and additional whites (based on Ca, Ti, Pb) than Ripolin paints. Interestingly, Ripolin paints produced in the United States showed a different composition based on both ZnO and TiO_2 as white pigments, with some extenders (small amounts of calcite and silicates), and, most importantly, both Pb and Fe impurities in the ZnO particles.

This is the first time that the nanoprobe has been used for the analysis of artists' paints, bridging the gap to the nanoscale of their multiscale characterization challenge.

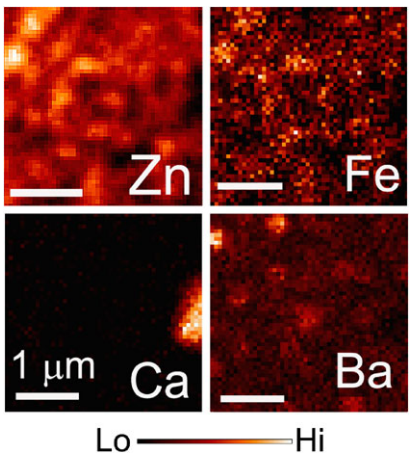

Fig. 8 Nano-XRF maps of a 3 × 3 μm^2 region in a sample of white paint and ground from Pablo Picasso's painting *Still Life with Three Fish, Moray Eel and Lime on White Ground*, 28 September 1946. The Ca- and Ba-rich particles are related to the composition of the ground, and the maps show excellent correlation between the Zn and Fe distribution

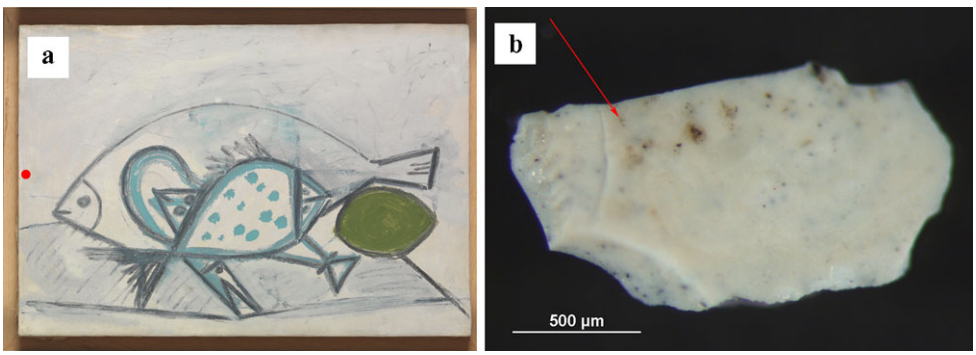

Fig. 9 (**a**) Pablo Picasso, *Still Life with Three Fish, Moray Eel and Lime on White Ground*, 28 September 1946 (oleoresinous enamel paint and charcoal on reused canvas, 38 × 55 cm^2, Musée Picasso, Antibes, France 1946.1.15) © Estate of Pablo Picasso / Artists Rights Society (ARS), New York: the *red dot* indicates where the sample illustrated in (**b**) was taken. (**b**) Micrograph of the sample of paint from (**a**): the red arrow shows the thin uppermost layer of house paint, which could not be mechanically separated from the thick ground layer below (sample courtesy C2RMF, Paris, France)

The results obtained might be valuable to elucidate the diverse range of luminescence properties of various zinc-based white pigments recently described in the literature, and the methodology will certainly be of interest for the study of a variety of other filled polymer systems as well as possible provenancing of historical mineral pigments. Future work will include analysis of paint samples as thin sections on transmission electron microscopy (TEM) grids, to avoid signals from buried layers; examination of additional representative examples of American process Zn white to confirm whether higher levels of impurities are consistently present when compared to the French process; and the correlation of SR-nanoprobe elemental mapping with synchrotron luminescence microspectroscopy on the same ZnO particles from this important historical paint set.

Acknowledgements Jerald Kavich and Gwénaëlle Gautier are gratefully acknowledged for assistance with the experimental work. Anna Vila is thanked for STEM images of zinc white paints; John Delaney and Michael Palmer at the National Gallery, Washington DC, for SEM/EDX images; and Mathieu Thoury for preliminary luminescence measurements. Michael Skalka, also of the National Gallery, Washington DC, is thanked for providing a sample of American Ripolin. Jean-Louis Andral (Musée Picasso Antibes), Gilles Barabant and colleagues (C2RMF) are gratefully acknowledged for the availability of the Antibes sample. Kimberley Muir is thanked for research on historical production of Zn oxide. Use of the Advanced Photon Source and the Center for Nanoscale Materials, Office of Science User Facilities operated for the U.S. Department of Energy (DOE) Office of Science by Argonne National Laboratory, was supported by the U.S. DOE under Contract No. DE-AC02-06CH11357. Scientific research at the Art Institute of Chicago is generously supported by the A.W. Mellon Foundation, the Grainger Foundation, the Barker Welfare Foundation, and the Stockman Family Foundation.

References

1. J.K. Delaney, J.G. Zeibel, M. Thoury, R. Littleton, M. Palmer, K.M. Morales, E.R. de la Rie, A. Hoenigswald, Appl. Spectrosc. **64**, 584 (2010)
2. G.S. Hall, J. Tinklenberg, J. Anal. At. Spectrom. **18**, 775 (2003)
3. K. Trentelman, M. Bouchard, M. Ganio, C. Namowicz, C.S. Patterson, M. Walton, X-Ray Spectrom. **39**, 159 (2010)
4. M. Alfeld, K. Janssens, J. Dik, W. de Nolf, G. van der Snickt, J. Anal. At. Spectrom. **26**, 899 (2011)
5. F. Casadio, L. Toniolo, J. Cult. Herit. **2**, 71 (2001)
6. S.E.J. Bell, L.A. Fido, S.J. Speers, W.J. Armstrong, S. Spratt, Appl. Spectrosc. **59**, 1340 (2005)
7. L. Burgio, R.J. Clark, Spectrochim. Acta Part A **57**, 1491 (2001)
8. I.M. Bell, R.J.H. Clark, P.J. Gibbs, Spectrochim. Acta Part A **53**, 2159 (1997)
9. M. Cotte, J. Susini, J. Dik, K. Janssens, Acc. Chem. Res. **43**, 705 (2010)
10. L. Monico, G. Van der Snickt, K. Janssens, W. De Nolf, C. Miliani, J. Verbeeck, H. Tian, H. Tan, J. Dik, M. Radepont, M. Cotte, Anal. Chem. **83**, 1214 (2011)
11. L. Monico, G. Van der Snickt, K. Janssens, W. De Nolf, C. Miliani, J. Dik, M. Radepont, E. Hendriks, M. Geldof, M. Cotte, Anal. Chem. **83**, 1224 (2011)
12. W.C. McCrone, J.G. Delly, S.J. Palenik, *The Particle Atlas: An Encyclopaedia of Small Particle Identification*. Light Microscopy Atlas and Techniques, vol. 5 (Ann Arbor Science, Ann Arbor, 1979)
13. J.L. Provis, V. Rose, S.A. Bernal, J.S.J. van Deventer, Langmuir **25**, 11897 (2009)
14. D. Comelli, A. Nevin, A. Brambilla, I. Osticioli, G. Valentini, L. Toniolo, M. Fratelli, R. Cubeddu, Appl. Phys. A **106**, 25 (2012)
15. M. Thoury, J.-P. Echard, M. Réfrégiers, B. Berrie, A. Nevin, F. Jamme, L. Bertrand, Anal. Chem. **83**, 1737 (2011)
16. S.H. Mousavi, H. Haratizadeh, H. Minaee, Opt. Commun. **284**, 3558 (2011)
17. R.L. Feller (ed.), *Artists' Pigments, Vol. 1: A Handbook of Their History and Characteristics* (Cambridge University Press, Cambridge, 1987)
18. ANON, L'écho Des Peintres (1909)
19. A.C. Downs, Bull. Assoc. Preserv. Technol. **8**, 80 (1976)
20. Picasso Express (Musée Picasso, Antibes, 2011)
21. K. Muir, G. Gautier, F. Casadio, A. Vila, in *ICOM Commitee for Conservation Preprints* (Critério—Artes Gráficas, Lda, Lisbon, 2011) (CD-ROM)
22. G. Gautier, A. Bezur, K. Muir, F. Casadio, I. Fiedler, Appl. Spectrosc. **63**, 597 (2009)
23. N. Heaton, *Outlines of Paint Technology*, 3rd edn. (Charles Griffin & Co., London, 1947). Thoroughly Revised, Etc.
24. C.T. Morley-Smith, J. Oil Colour Chem. Assoc. **41**, 85 (1958)
25. M. Fauve, J. Vandemaele, in *Contributions to the 7th FATIPEC Congress in Vichy* (Fédération d'Associations de Techniciens des Industries des Peintures, Vernis, Emaux et Encres d'Imprimerie de l'Europe Continentale, Paris, 1964), pp. 233–244
26. R.P. Winarski, M.V. Holt, V. Rose, F. Fuesz, D. Carbaugh, C. Benson, D. Shu, G.B. Stephenson, I. McNulty, J. Maser, J. Synchrotron Radiat. **19**, 1056 (2012)
27. S. Vogt, J. Phys. IV **104**, 635 (2003)
28. S. Vogt, personal communication. Data measured at beamline 2-ID-E of the Advanced Photon Source at Argonne National Laboratory
29. B.L. Henke, E.M. Gullikson, J.C. Davis, At. Data Nucl. Data Tables **54**(2), 181–342 (1993)